

Article ID: 1006-8775(2022) 02-0252-9

## A Brief Discussion on the High-impact Cold-season Tornado Outbreak During 10–11 December 2021 in the United States

LI Cai-ling (李彩玲)<sup>1</sup>, BAI Lan-qiang (白兰强)<sup>1,2</sup>, YU Xiao-ding (俞小鼎)<sup>3</sup>, TAN Hao-bo (谭浩波)<sup>4</sup>, HUANG Xian-xiang (黄先香)<sup>1</sup>, YAN Li-jun (炎利军)<sup>1</sup>, LI Zhao-ming (李兆明)<sup>1</sup>, ZHANG Ze-yu (张泽宇)<sup>1</sup>

1. Foshan Tornado Research Center, Foshan Meteorological Service, Foshan, Guangdong 528000 China;
2. Southern Marine Science and Engineering Guangdong Laboratory (Zhuhai), Zhuhai, Guangdong 519082 China;
3. China Meteorological Administration Training Center, Beijing 100081 China;
4. Guangdong Meteorological Service, Guangzhou 510062 China)

**Abstract:** An outbreak of powerful tornadoes tore through multiple states in the central and southern United States from 10 to 11 December 2021. It is claimed the deadliest tornado outbreak that has taken place on December days. The National Oceanic and Atmospheric Administration had confirmed 66 tornadoes as of 21 December, producing at least 90 fatalities. Most tornadoes occurred at night and thus they were difficult to be visually located, which directly increases the risk for local residents. Two violent nighttime tornadoes were rated category 4 on the enhanced Fujita scale (EF4). Although a high death toll was caused during this event, the operational service actually presented an excellent performance. This tornado outbreak has aroused extensive discussion from both the public and the research community in China. This paper presents a brief discussion on the formation environment and warning services of the tornado outbreak. Recall the deadliest violent tornado in the past 45 years in China, the radar-based tornadic vortex signatures at the locations with EF4 damages show a comparable strength with those in the current cases. Some views on the tornado warning issuance and receiving and damage surveys in China are also presented.

**Key words:** tornado; tornado outbreak; severe weather; cold season; warning service

**CLC number:** P44      **Document Type:** News and Views

**Citation:** LI Cai-ling, BAI Lan-qiang, YU Xiao-ding, et al. A Brief Discussion on the High-impact Cold-season Tornado Outbreak During 10-11 December 2021 in the United States [J]. Journal of Tropical Meteorology, 2022, 28(2): 252-260, <https://doi.org/10.46267/j.1006-8775.2022.019>

### 1 OVERVIEW AND FORMATION ENVIRONMENT OF THE TORNADO OUTBREAK

Tornadoes are violently rotating columns of air that usually manifest themselves as funnel-shaped clouds extending downward from the thunderstorm base to the ground (Markowski and Richardson<sup>[1]</sup>). They threaten human lives by producing very high winds at surface. Violent tornadoes that are rated EF4 or EF5 on the enhanced Fujita scale are particularly deadly because they can generate destructive wind gusts exceeding 75 m s<sup>-1</sup> (EF4) or 90 m s<sup>-1</sup> (EF5). Statistics in the United States show that tornadoes occurring from local

midnight to sunrise are more deadly compared to those occurring during the daytime (Ashley et al.<sup>[2]</sup>). These nocturnal tornadoes tend to take place in winter and are most prevalent in the central and southeast United States. During 10–11 December 2021, an outbreak of powerful nocturnal tornadoes tore through multiple states in the central and southern parts of the United States. It has aroused widespread attention from both the public and the research community in China. According to the National Weather Service (NWS) of National Oceanic and Atmospheric Administration (NOAA), 66 tornadoes were confirmed with several violent ones rated EF4 during this event as of 21 December 2021, producing catastrophic damage with a death toll of 90 (NOAA<sup>[3]</sup>). It is not the only tornado outbreak that takes place on December days on record in the United States, but it is the deadliest one based on NOAA's tornado database since 1950. The authors would like to extend our deepest condolences to the people who lost their lives in this severe weather event.

A synoptic-scale meteorological analysis suggests that the tornado outbreak occurred from frontal systems that were associated with an extratropical cyclone (refer to the low-pressure region indicated by the isopleths in Fig. 1a) located downstream of a deep midlevel trough (refer to the heavy curve in Fig. 1a). Previous studies

**Submitted** 2022-02-15; **Revised** 2022-03-15; **Accepted** 2022-05-15

**Funding:** Radar Application and Short-term Severe-weather Predictions and Warnings Technology Program (GRMCTD202002); Foshan Innovation Driving and Assistance Project (2021002); Science and Technology Planning Project of Guangdong Province (2019B020208015); Foshan Science and Technology Project in Social Field (2120001008761)

**Biography:** LI Cai-ling, Senior Engineer, primarily undertaking research on severe convective weather.

**Corresponding author:** BAI Lan-qiang, e-mail: [bailanqiang@foxmail.com](mailto:bailanqiang@foxmail.com)

have documented that extratropical cyclones are one of the favorable synoptic environments for tornado outbreaks (e. g., Newton [4]; Barnes and Newton [5]; Tochimoto et al. [6]). In the lower troposphere, notable warm airmasses from southeast and cold airmasses from northwest collided in the central U.S. (Fig. 1b), creating a baroclinic environment that favors the extratropical cyclone development. The clash of cold and warm air

masses is not directly related to the tornadogenesis (Schultz et al. [7]) but the unstable atmospheric conditions with strong vertical wind shear around the frontal zone bring together the ingredients for the formation of the widespread southwest-northeast-oriented storms over the east portion of the extratropical cyclone (Fig. 1c).

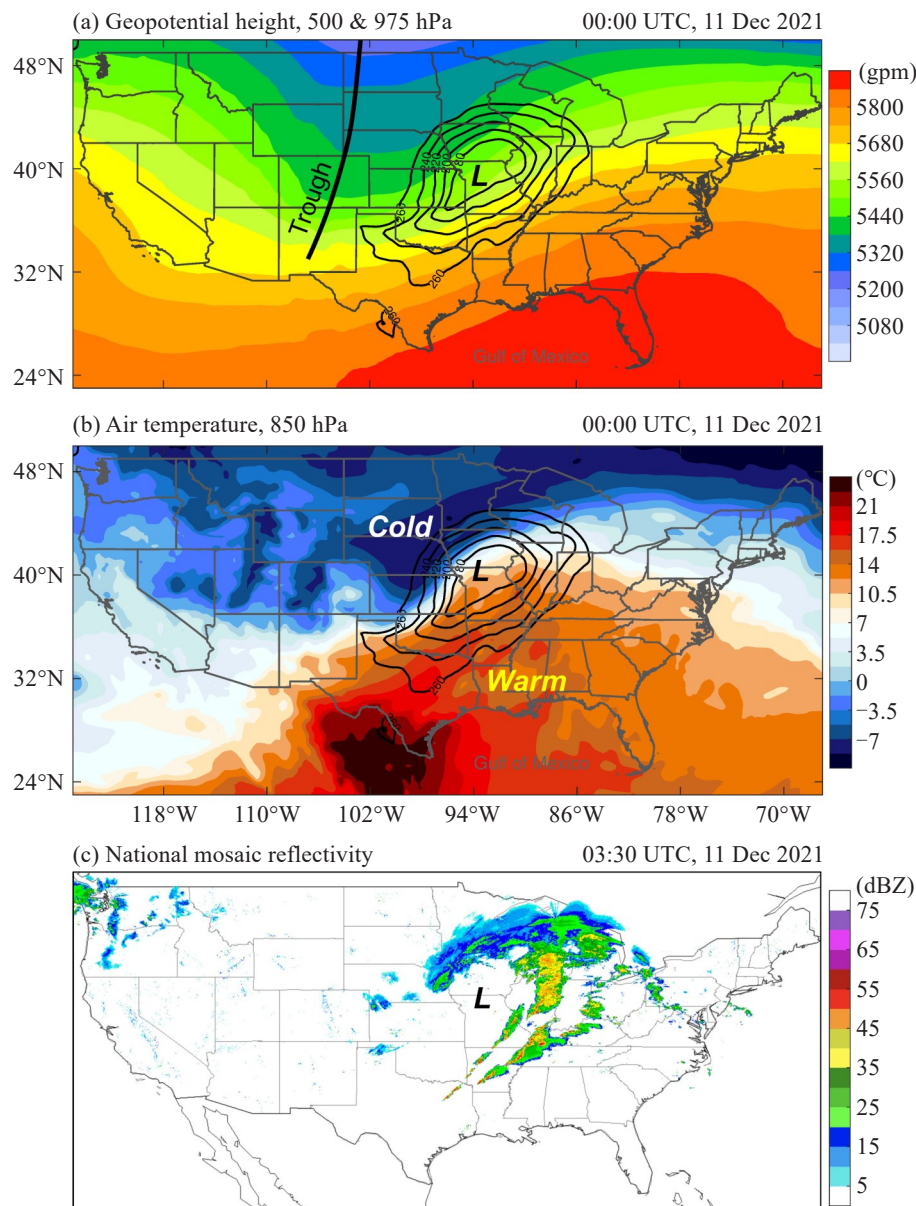


**Figure 1.** (a) Geopotential heights on 500 hPa (shaded) and 975 hPa (contoured from 180 to 260 gpm). The rough location of the extratropical cyclone center is labeled L. The thick black curve denotes the 500-hPa trough. (b) Upper-air temperature on 850 hPa (shaded). The calculations for (a) and (b) are based on the ERA5 reanalysis data. (c) Screenshot of the national mosaic reflectivity obtained from the NOAA/NCEI website (<https://www.ncei.noaa.gov/maps/radar/>).

Located to the southeast of the extratropical cyclone, the central and southern U.S. was characterized by high mixed-layer (lowest 1 km above the ground level) convective available potential energy (CAPE) and high 0-1 km storm relative helicity (SRH) (Figs. 2a and

b). The supercell composite parameter (SCP) is usually used to identify environments supporting supercells. It combines measures of buoyancy, helicity and vertical wind shear. Fig. 2c shows that the region of interest features large SCP values (greater than 1), indicating

that the atmosphere over there supports the supercellular organization for any relatively isolated storms. The ingredients-based significant tornado parameter (STP) that is often used to aid operational forecasters in

discriminating between significantly tornadic and nontornadic supercell environments exerts high values in the central and southern U.S., suggesting a high risk of significantly tornadic supercells (Fig. 2d).

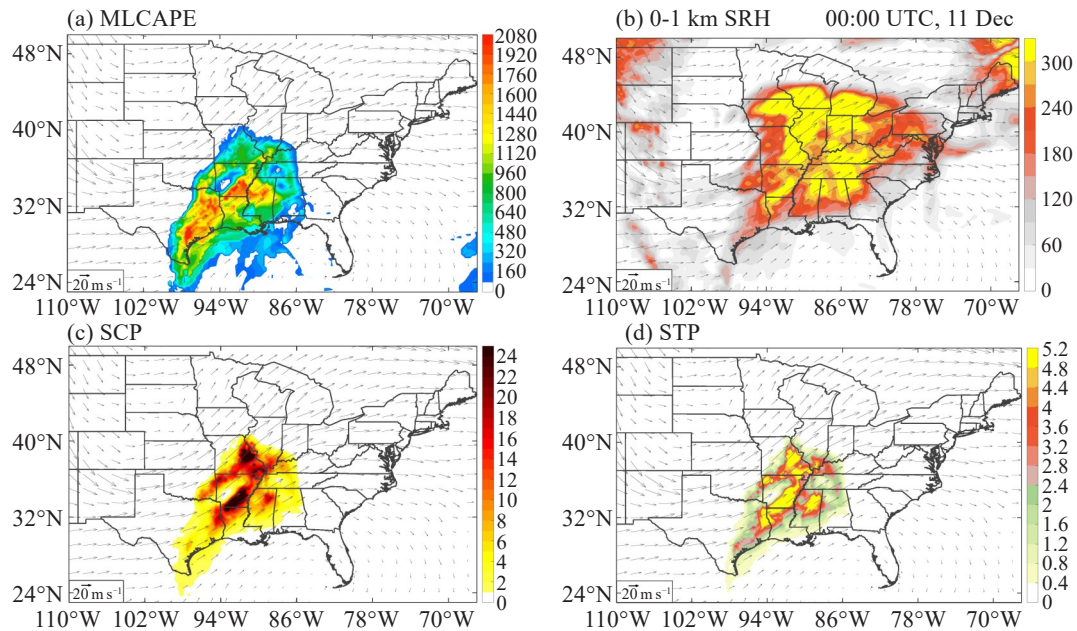


**Figure 2.** (a) Mixed-layer convective available potential energy (MLCAPE; units:  $\text{J kg}^{-1}$ ), (b) 0–1-km storm relative helicity (SRH; units:  $\text{m}^2 \text{s}^{-2}$ ), (c) supercell composite parameter (SCP), and (d) significant tornado parameter (STP). All parameters were calculated from the ERA5 reanalysis data at a horizontal resolution of  $0.25^\circ$  (Hersbach et al. [29]) valid at 00:00 UTC on 11 December 2021. The vectors represent the 500-hPa horizontal winds.

The unusually warm air in the lower troposphere in this December is noticeable. Over the southern part of the United States, the surface is exceptionally warm with a daily average of 2-m temperature generally exceeding  $15^\circ\text{C}$  on December 10 (Fig. 3a). Compared to the mean atmospheric conditions on December days from 1979 to 2021, a large portion of the southern U.S. was characterized by positive anomaly of 2-m temperature as high as at least  $8^\circ\text{C}$ , suggesting abnormally warm December days in 2021 (Fig. 3b). Such a warm lower troposphere is likely a result of the warmer sea surface compared to the mean climate over the North Atlantic Ocean, especially over the Gulf of Mexico (Fig. 3c). Warmer low-level temperature tends to increase the lapse rate and thus create large conditional instability supporting convective updrafts. In fact, the entire December in 2021 is exceptionally warm (Fig. 3d). An additional extratropical cyclone produced another tornado outbreak during December 15–16, leaving at least 94 tornadoes from the central Plains to the Upper Midwest and Great Lakes (NOAA [8]). Iowa was hit by at least 63 tornadoes as of 4 January 2022, 21 of which were rated EF2 (NOAA [9]). Although the unusually warm lower troposphere was an important ingredient in

both tornado outbreaks during December 10–11 and 15–16, it is not that simple to conclude that the outbreaks are directly associated with climate change just based on these two cases.

Confirmed from the ground-based radar observations during the December 10–11 outbreak, multiple discrete supercells within this large-scale quasi-linear convective rainband are responsible for the tornado outbreak on storm scale. Supercells have rotating updrafts due to strong vertical wind shear and are the most common type of thunderstorm responsible for destructive tornadoes (Markowski and Richardson [1]). According to the surveyed tornado damage summaries by NWS as of 21 December, 2021, two EF4 and six EF3 tornadoes were rated (NOAA [3]). Among them, two EF4 and two EF3 tornadoes were produced by supercells with well-defined hook-echo signatures (Fig. 4a and Figs. 5a, c, and g). Three cases (two EF4 and one EF3) had a peak-strength tornadic vortex signature (TVS) exceeding  $85 \text{ m s}^{-1}$  at the lowest radar level in terms of maximum gate-to-gate storm-relative radial velocity<sup>1</sup> (SRV) difference (Fig. 4c and Figs. 5d, e). The rest five EF3 tornadoes were characterized by a peak lowest-level TVS less than  $60 \text{ m s}^{-1}$  (Figs. 5f and 5j-l). Despite the fact that strong low-level TVVs typically are related to violent tornadoes, some relatively weak azimuthal rotational signatures can

<sup>1</sup> The storm-motion vector that was used to calculate storm-relative radial velocity was estimated by tracking the centroid of velocity couplet signature of a given storm.

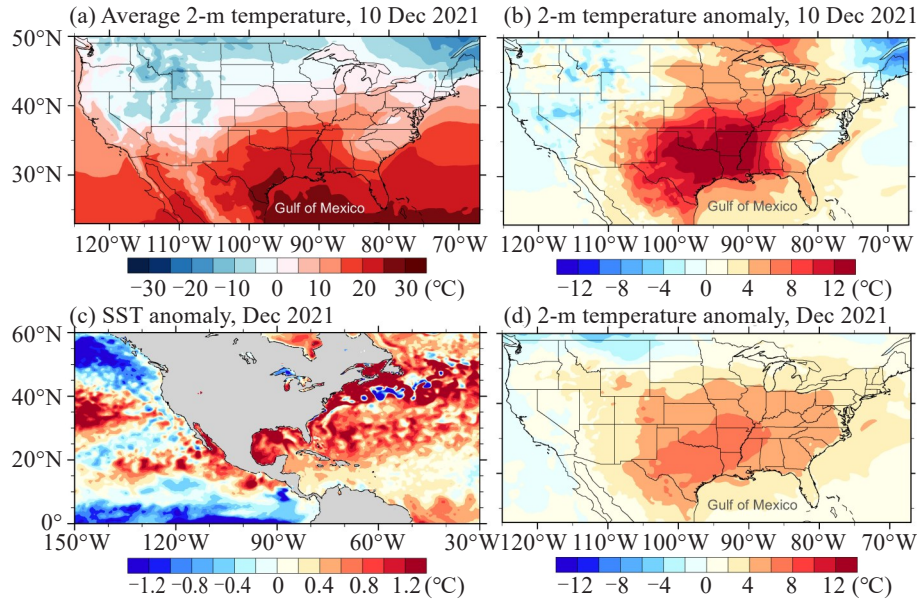


**Figure 3.** (a) Daily average of 2-m temperature on 10 December 2021. (b) Anomaly of daily average 2-m temperature on 10 December 2021 compared to the mean atmospheric conditions on December days from 1979 to 2021. (c) Anomaly of sea surface temperature (SST) compared to the mean climate from 1979 to 2021. (d) Anomaly of average 2-m temperature in the entire December in 2021 compared to the mean climate in Decembers from 1979 to 2021. All calculations were conducted based on the ERA5 reanalysis data.

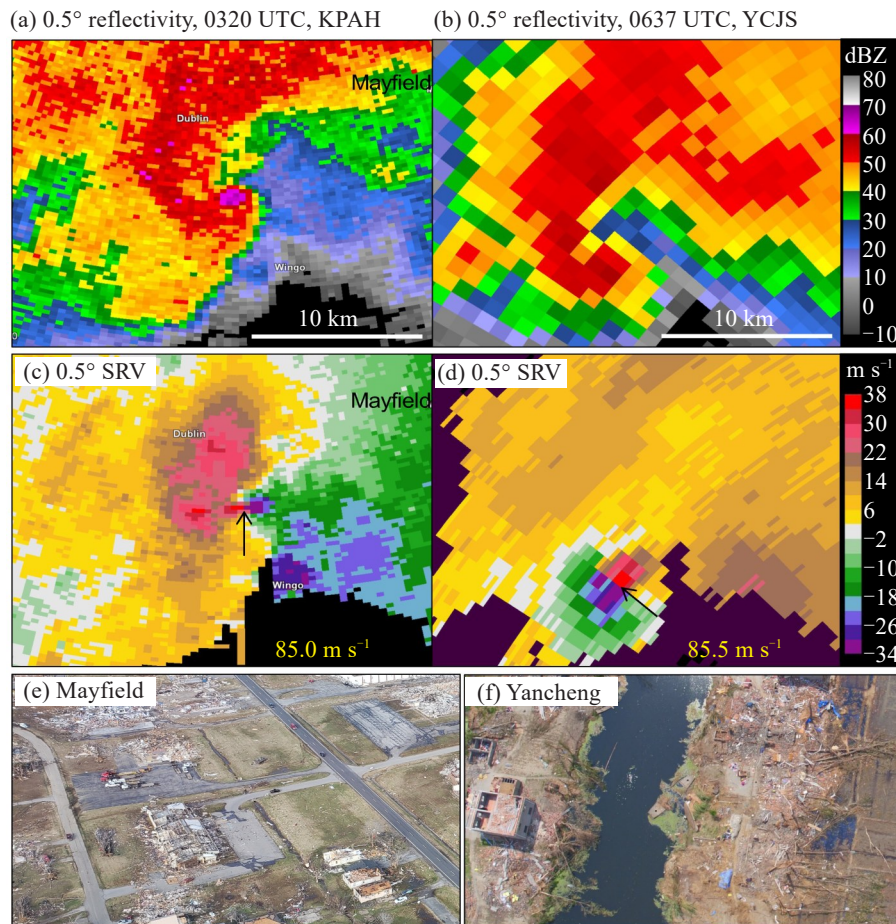


**Figure 4.** (a), (b) Reflectivity and (c), (d) storm-relative radial velocity (SRV) for the (left) KPAH radar (USA) on 11 December 2021 and (right) YCJS radar (China) on 23 June 2016. The maximum gate-to-gate SRV differences (denoted by the arrows) are denoted by the numbers at the bottom-right corner in (c) and (d). Snapshots of aerial photo of damage near (e) Mayfield, KY (downloaded from the NOAA NWS website available online at <https://www.weather.gov/pah/December-10th-11th-2021-Tornado>) and (f) Yancheng city, Jiangsu Province.

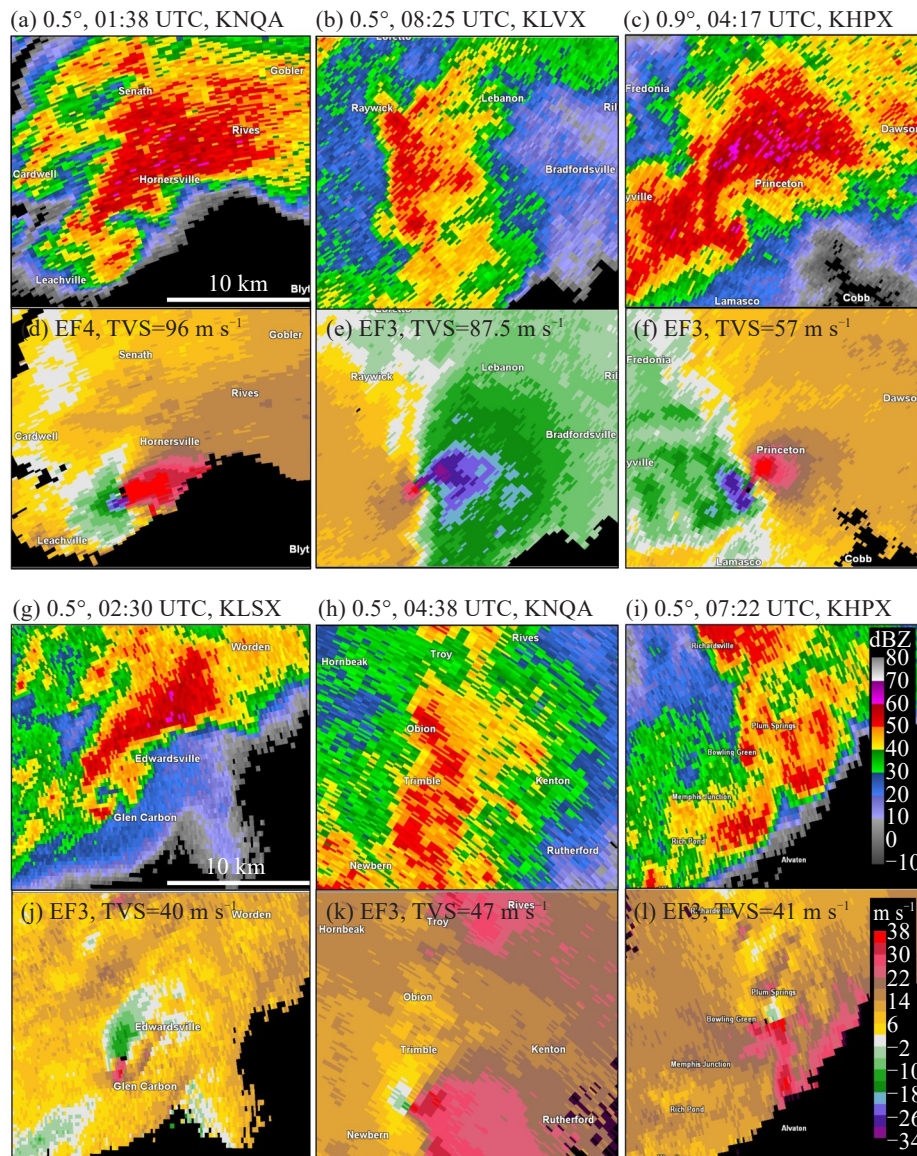


**Figure 5.** (a)-(c), (g)-(i) Reflectivity and (d)-(f), (j)-(l) storm-relative radial velocity (SRV) of some EF3/EF4 tornadic storms during the December 10–11 tornado outbreak. The selected time for each case corresponds to the peak TVS strength. The elevation angle and radar site are also labeled in the subtitle. The color scales for reflectivity and SRV are presented in (i) and (l), respectively.

also correspond to high EF-scale damage ratings (e. g., Smith et al. <sup>[10]</sup>; Thompson et al. <sup>[11]</sup>). During the outbreak, several supercells exhibited a long-lived nature, leaving several long-track tornadoes, which was one of the extraordinary aspects of this cold-season tornado outbreak. The maximum length of the ground damage path reached up to 267 km (165.7 miles) left by an EF4 tornado across Tennessee and Kentucky (NOAA <sup>[12]</sup>). The longest track of record to date is the “Tri-state” tornado of 18 March 1925, with an officially accepted damage path of 352 km (219 miles) long (Grazulis <sup>[13]</sup>; Johns et al. <sup>[14]</sup>). It is worth mentioning that the “Tri-state” tornado also formed ahead of an extratropical cyclone causing a death toll of 695 (Doswell and Burgess <sup>[15]</sup>; Johns et al. <sup>[14]</sup>).

<sup>2</sup> Scattered severe storms possible.

## 2 WARNING SERVICES OF THE TORNADO OUTBREAK

Despite the heavy casualties during this severe weather event, the U.S. operational warning service presented an excellent performance in regards of convective outlook, tornado watch, and tornado warning. At 08:15 UTC (UTC = Central Standard Time + 6 h) on December 8, the NOAA / NWS Storm Prediction Center (SPC) issued a convective outlook for the period from 12:00 UTC December 10 to 12:00 UTC December 11 (Fig. 6a), forecasting a SLIGHT<sup>2</sup> category of severe thunderstorm risk with a probability of 15% in the central-to-southeast U.S. area covering ten states (about 3 days prior to the first tornado occurrence; NOAA <sup>[16]</sup>). On December 9, the SPC issued an increased

severe thunderstorm risk (ENHANCED<sup>3</sup> category) for the same period around this region. Meanwhile, a tornado outlook was issued, showing this high thunderstorm risk region was also faced with an EF2-EF5 tornado threat with a probability of at least 10% (about 2 days prior to the first tornado occurrence; Fig. 6a). At 16:18 UTC on December 10, the updated probability of this tornado threat increased to 15% covering parts of Tennessee, Arkansas, Missouri, Kentucky, Illinois and Indiana (about 8 h prior to the first tornado occurrence; Figs. 6a and b). According to the tornado statistics from 1950 to 2005, this area is characterized by a high percentage of nocturnal tornadoes with more than 40% nocturnal tornadoes in Tennessee, Arkansas and Kentucky and more than 30% in Missouri, Indiana and southern part of Illinois (Fig. 6 in Ashley et al.<sup>[2]</sup>). At 21:00 UTC on this day, the SPC issued the first tornado watch across the aforementioned high-risk area, stating that scattered supercells were expected and a likely occurrence of several tornadoes

and a couple of intense tornadoes from that afternoon to 05:00 UTC on December 11 (about 3 h prior to the first tornado occurrence; Fig. 6a). At 23:51 UTC on December 10, the NWS office in North Little Rock issued the first tornado warning associated with a supercell storm in Arkansas (about 15 min prior to the first tornado occurrence). Actually, there were more than 100 tornado warnings being issued throughout the night of December 10 across portions of nine states over the high-risk area. The SPC received the first tornado report (22:12 UTC on December 10) around the Tallapoosa Lakes in Alabama (please refer to the red triangle in circle in Fig. 6c) which is located out of the aforementioned tornado high risk area (this tornado is thus excluded in this study). The first reported tornado located within the high-risk area occurred in the northern portion of Arkansas at around 00:06 UTC on December 11. During the two-day outbreak event, the SPC received a total of 106 filtered tornado reports with 102 reports for 10 December and 4 reports for 11 December (Fig. 6c).

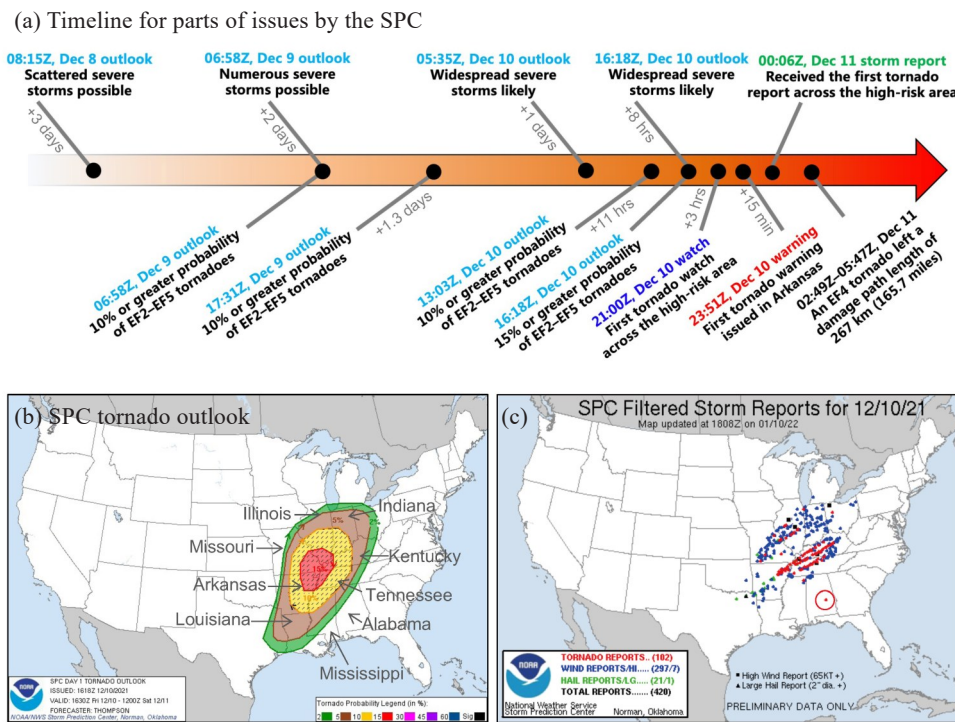


**Figure 6.** (a) Timeline for parts of issues by the NOAA/NWS SPC. (b) SPC tornado outlook issued at 16:18 UTC on 10 December 2021 valid from 16:30 UTC 10 December to 12:00 UTC 11 December. (c) SPC filtered storm reports for 10 December 2021. The base maps in (b) and (c) are obtained from the NOAA website (<https://www.spc.noaa.gov/>).

Known as Integrated Warning System, a complete tornado warning process involves sequential complex procedures including forecast, detection, warning decision, dissemination, and public response (Doswell et al.<sup>[17]</sup>; Brotzge and Donner<sup>[18]</sup>). The tornado warnings can be issued based on observational (warn-on-detection) and modeling (warn-on-forecast; Stensrud et

<sup>3</sup> Numerous severe storms possible.

al.<sup>[19]</sup>) analysis. A visual tornado evidence that is timely reported by volunteer storm spotters (SKYWARN Storm Spotter Program; Doswell et al.<sup>[17]</sup>) would make it easier for making warning decision because sometimes a tornado occurrence may be hard to be inferred from radar observations. To stay safe from destructive tornadoes, timely and efficient dissemination of warning information, the public risk awareness, and associated

quick behavioral response are indispensable in addition to successful severe weather forecasting and warning services. For nighttime tornadoes like those occurred during this event, they can be particularly deadly due to a potential receiving failure of issued warnings when local residents are asleep. An earlier alert for such nighttime tornadoes is especially beneficial relative to the daytime ones given that funnel clouds are difficult to be spotted in the dark and thus people need more time to find safe shelters.

### 3 SOME VIEWS ON THE TORNADO WARNING IN CHINA

China is also faced with tornado threats despite a much smaller number of occurrence in contrast with the United States (Fan and Yu<sup>[20]</sup>; Bai et al.<sup>[21]</sup>; Yao et al.<sup>[22]</sup>). According to the data provided by Dr. Zhiyong Meng from Peking University, National Meteorological Center, and Foshan Tornado Research Center, a total of 236 reported tornadoes on land (i. e., landspouts) were confirmed (Li et al.<sup>[23]</sup>; Zhi et al.<sup>[24]</sup>) over the period of 2016–2021 in the Chinese mainland with an annual average of 39. Waterspouts (i. e., tornado over a body of water) were not included in the calculation because 46 waterspouts were recorded in 2021 while much fewer waterspouts were reported in earlier years, indicative of a possible underestimation of waterspout records during those years. In the last year (2021), tornadoes caused a death toll of 23. The deadliest tornado in the past 45 years in China, known as the 2016 Yancheng EF4 tornado, caused 98 fatalities in Funing county, Yancheng city, Jiangsu Province (Meng et al.<sup>[25]</sup>). Figs. 4a-d present a comparison of the lowest-level radar reflectivity and storm-relative radial velocity between the supercell for the 2016 Yancheng EF4 tornado and a tornadic supercell in the current tornado outbreak event. The hook echoes of these two supercells were both located approximately 45–50 km from radar sites. At the selected times as shown in Fig. 4, the maximum gate-to-gate SRV differences (marked by arrows in Figs. 4c and d) of the two supercells are both approximately  $85 \text{ m s}^{-1}$ . Near these TVSSs, EF4 damages (total destructions of entire well-constructed buildings) were identified on the ground (e. g., Figs. 4e, f). In eastern China, the tornado-prone zones are typically located in relatively flat regions, especially in coastal provinces (Fan and Yu<sup>[20]</sup>). Heavy fatality tends to occur because these areas are highly populated. On the other hand, it is noteworthy that supercells in this climate regime are usually characterized by high precipitation and thus a well-defined hook echo signature is often hard to recognize. Owing to the widely used smartphones and social media in recent years, the public's increasing awareness of tornado would largely benefit the future tornado warning service and the subsequent public response.

Given the burst nature of tornado, an efficient, fast,

and audience-targeted warning dissemination system is warranted for disaster prevention and mitigation. Considering that power may go out at any moment and mobile communication base stations may be destroyed and thus smartphone services can be unavailable, multiple energy-storage broadcast devices are critical for reliably receiving tornado warnings in addition to the typical online warning services through smartphone-based message warning, television, websites of meteorological agencies, and social media (e. g., Sina Weibo, Douyin, WeChat Moments, etc.). In the United States, the outdoor warning sirens play an important role in tornado alert. Indoors, the widely adopted NOAA Weather Radio (NWR) is one of effective methods for waking a person from sleep at home. It is like a smoke detector for severe weather. In the NWR “standby” or “alert” mode, alert tone will be activated if an alerting message is received. This method may not work in China because in-home radios are barely used. The pre-deployed outdoor loudspeakers for emergency alarm may be one of the good offline devices if they are equipped with batteries. People are also easily being alerted by these loudspeakers. Although these loudspeakers are easily available, they may still be not effective enough due to the limited covering area. Unmanned aerial vehicles (UAV) carrying speakers are an alternative convenient tool given their mobility advantage to fast reach the targeted area. During the COVID-19 pandemic, some community services in China have adopted such a method for broadcasting anti-epidemic measures to minimize physical contact. Recently, the UAV speakers have also been used to solve the traffic jam problems in some large cities.

Meanwhile, a tornado warning decision is largely dependent on the accurate tornado monitoring primarily by Doppler weather radars. Eastern China has started to deploy multiple dual-polarization phased-array weather radars (dual-PAWRs), especially in the Greater Bay area including Guangdong, Hong Kong and Macau which is one of the tornado-prone zones. The dual-PAWR network with rapid-scan strategy and super-high sampling resolution provides new opportunities to monitor supercellular storms and assess their attendant tornado risk in the Greater Bay area (Zhang et al.<sup>[26]</sup>). This dual-PAWR network-based tornado warning system may make earlier alerts for tornadoes possible. For these new advanced devices, corresponding updated automated detection algorithms, such as the mesocyclone and tornado detection algorithms, are urgently demanded for automatically identifying radar-based tornado features in real time. After a long-term collection of supercell observations, statistics of polarimetric signatures may lend support to assessing the discriminatory potential between tornadic and nontornadic supercells under specific regional climate (Kumjian et al.<sup>[27]</sup>; Loeffler et al.<sup>[28]</sup>).

Another issue is the demand for qualified volunteer

storm spotters as many as possible. The radar-based algorithms may miss a tornado that has occurred. Onsite tornado reports from widespread storm spotters will be helpful for gaining extra time for the downstream public and supporting timely emergency response. Some violent tornadoes often have a relatively long lifespan. For instance, the 2016 Yancheng EF4 tornado lasted for approximately 50 min. The radar-based tornado detection algorithms failed to alert a tornado during the early stage of this violent tornado. The lowest-level radial velocities around the tornado location looks chaotic due to the velocity aliasing issues, which makes it difficult to identify any tornado vortex signature in real-time even for experienced forecasters. The algorithms alerted a tornado occurrence about 16 min after the actual tornadogenesis. A timely tornado report from storm spotters near the storms of interest would give forecasters more confidence to issue a tornado warning at tornado's earlier stage.

After a (possible) tornado event, ground damage surveys are urgently needed to confirm the occurrence of tornado and/or estimate the tornado strength by assigning a degree of damage to a ground damage indicator. In practice, however, it is often difficult to timely achieve that goal because of the rescue and recovery needs. Things will be especially difficult during a major tornado outbreak in which multiple tornadoes are likely to be distributed in a wide range of area, like the situation during the current event. Onsite damage surveys usually take a long time. A survey team needs to repeatedly drive from the office to the damage path in days, especially during a long-track tornado event. Sometimes vehicles are even not allowed due to damage obstacles. A lot of time is required to identify and locate damage indicators after having confirmed the damage-inducing weather system (e.g., tornado or downburst). Interviewing the local residents and gathering videos and photos associated with the damaging weather system are also time-consuming routines. Many efforts will be put into analyzing the massive survey data, including the GPS coordinates and photos of damage indicators, and pinpointing the damage information on maps. To timely achieve these procedures, survey teams organized by local meteorological agencies are most suitable. Therefore, nationwide popularizing the professional damage survey strategy is important, especially when faced with an abrupt outbreak event. A new, experimental three-dimensional reconstruction of the damaging scene is now conducted through the photography techniques by multiple drones. This strategy aims to rapidly and efficiently provide three-dimensional clear views of ground damages. May these efforts facilitate a faster response to the unexpected disaster incidents of severe weather in the future.

**Acknowledgments:** The online information on the tornado outbreak provided by the NOAA/NWS and NOAA/SPC, and

the ERA5 reanalysis data provided by ECMWF are gratefully acknowledged. The authors would like to thank the anonymous reviewers for their valuable comments.

## REFERENCES

- [1] MARKOWSKI P, RICHARDSON Y. Mesoscale Meteorology in Midlatitudes [M]. Wiley-Blackwell, Wiley, New York, 2010: 407 pp.
- [2] ASHLEY W S, KRMENEC A J, SCHWANTES R. Vulnerability due to nocturnal tornadoes [J]. *Weather and Forecasting*, 2008, 23(5): 795-807, <https://doi.org/10.1175/2008WAF2222132.1>
- [3] NOAA. NWS Storm Damage Summaries [J/OL]. <https://www.weather.gov/crh/dec112021>, 2022-02-10.
- [4] NEWTON C W. Severe convective storms [J]. *Advances in Geophysics*, 1967, 257-303, [https://doi.org/10.1016/S0065-2687\(08\)60377-5](https://doi.org/10.1016/S0065-2687(08)60377-5)
- [5] BARNES S L, NEWTON C W. Thunderstorms in the synoptic setting [M]// KESSLER E, *Thunderstorm Morphology and Dynamics*. Norman: University of Oklahoma, 1983: 75-112.
- [6] TOCHIMOTO E, NIINO H. Structural and environmental characteristics of extratropical cyclones that cause tornado outbreaks in the warm sector: a composite study [J]. *Monthly Weather Review*, 2016, 144(3): 945-969. <https://doi.org/10.1175/MWR-D-15-0015.1>
- [7] SCHULTZ D M, RICHARDSON Y P, MARKOWSKI P M, et al. Tornadoes in the central United States and the "clash of air masses" [J]. *Bulletin of the American Meteorological Society*, 2014, 95, 1704-1712, <https://doi.org/10.1175/bams-d-13-00252.1>
- [8] NOAA. Historic, Unprecedented Storm of December 15-16, 2021 -- Updated Jan 27 -[J/OL]. <https://www.weather.gov/mpx/HistoricStormDecember2021>, 2022-02-10.
- [9] NOAA. Severe Storms and Extreme Winds - December 15, 2021 [J / OL]. <https://www.weather.gov/dmx/StormyandWindyWednesdayDecember152021>, 2022-02-10.
- [10] SMITH B T, THOMPSON R L, DEAN A R, et al. Diagnosing the conditional probability of tornado damage rating using environmental and radar attributes [J]. *Weather and Forecasting*, 2015, 30, 914-932.
- [11] THOMPSON R L, and COAUTHORS. Tornado damage rating probabilities derived from WSR-88D data [J]. *Weather and Forecasting*, 2017, 32(4): 1509-1528, <https://doi.org/10.1175/WAF-D-17-0004.1>
- [12] NOAA. Dec 10-11 2021 Tornado Event [J/OL]. <https://www.weather.gov/pah/December-10th-11th-2021-Tornado>, 2022-02-10.
- [13] GRAZULIS T P. Significant Tornadoes 1680-1991 [M]. *Environmental Films*, 1993: 1326 pp.
- [14] JOHNS R H, BURGESS D W, DOSWELL III C A, et al. The 1925 Tri-State tornado damage path and associated storm system [J]. *E-Journal of Severe Storms Meteorology*, 2013, 8(2): 1-33.
- [15] DOSWELL III C A, BURGESS D W. On some issues of United States Tornado climatology [J]. *Monthly Weather Review*, 1988, 116(2): 495-501, [https://doi.org/10.1175/1520-0493\(1988\)116<0495:OSIOUS>2.0.CO;2](https://doi.org/10.1175/1520-0493(1988)116<0495:OSIOUS>2.0.CO;2)
- [16] NOAA. SPC Convective Outlooks Issued Between 20211208 and 20211210 [J/OL]. <https://www.spc.noaa>



- gov/cgi-bin/spc/getacrange.pl?date0=20211208&date1=20211210, 2022-02-10.
- [17] DOSWELL III C A, MOLLER A R, BROOKS H E. Storm spotting and public awareness since the first tornado forecasts of 1948 [J]. *Weather and Forecasting*, 1999, 14(4): 544-557, [https://doi.org/10.1175/1520-0434\(1999\)014<0544:SSAPAS>2.0.CO;2](https://doi.org/10.1175/1520-0434(1999)014<0544:SSAPAS>2.0.CO;2)
- [18] BROTZGE J, DONNER W. The tornado warning process: A review of current research, challenges, and opportunities [J]. *Bulletin of the American Meteorological Society*, 2013, 94(11): 1715-1733, <https://doi.org/10.1175/BAMS-D-12-00147.1>
- [19] STENSRUD D J, XUE M, WICKER L J, et al. Convective-scale warn-on-forecast system [J]. *Bulletin of the American Meteorological Society*, 2009, 90(10): 1487-1499, <https://doi.org/10.1175/2009BAMS2795.1>
- [20] FAN W J, YU X D. Characteristics of spatial-temporal distribution of tornadoes in China [J]. *Meteorological Monthly (in Chinese)*, 2015, 41, 793-805.
- [21] BAI L Q, MENG Z Y, SUEKI K et al. Climatology of tropical cyclone tornadoes in China from 2006 to 2018 [J]. *Science China Earth Sciences*, 2020, 63, 37-51, <https://doi.org/10.1007/s11430-019-9391-1>
- [22] YAO D, LIANG X D, MENG Q, et al. Importance of identifying tropical cyclone tornadoes in typhoon warning and defense systems [J]. *Science Bulletin*, 2019, 64(3): 143-145, <https://doi.org/10.1016/j.scib.2018.12.022>
- [23] LI C L, TAN H B, CAI K L, et al. Tornadoes in China and their disaster characteristics from 2016 to 2020 [J]. *Journal of Tropical Meteorology (in Chinese)*, 2021, 37(5-6): 733-747, <https://doi.org/10.16032/j.issn.1004-4965.2021.068>
- [24] ZHI J L, HUANG X X, BAI L Q, et al. Tornadoes and associated ground damages in China in 2021 [J]. *Advances in Meteorological Science and Technology (in Chinese)*, 2022, 12(1): 26-36.
- [25] MENG Z Y, BAI L Q, ZHANG M R, et al. The deadliest tornado (EF4) in the past 40 years in China [J]. *Weather and Forecasting*, 2018, 33: 693-713, <https://doi.org/10.1175/WAF-D-17-0085.1>
- [26] ZHANG Y, BAI L Q, MENG Z Y, et al. Rapid-scan and polarimetric phased-array radar observations of a tornado in the Pearl River Estuary [J]. *Journal of Tropical Meteorology*, 2021, 27(1): 80-85, <https://doi.org/10.46267/j.1006-8775.2021.008>
- [27] KUMJIAN M R, RYZHKOV A V. Polarimetric signatures in supercell thunderstorms [J]. *Journal of Applied Meteorology and Climatology*, 2008, 47(7): 1940-1961, <https://doi.org/10.1175/2007JAMC1874.1>
- [28] LOEFFLER S D, KUMJIAN M R, JUREWICZ M, et al. Differentiating between tornadic and nontornadic supercells using polarimetric radar signatures of hydrometeor size sorting [J]. *Geophysical Research Letters*, 2020: 47(12): e2020GL088242, <https://doi.org/10.1029/2020GL088242>
- [29] HERBACH H, BILL B, BERRISFORD P, et al. The ERA5 global reanalysis [J]. *Quarterly Journal of the Royal Meteorological Society*, 2020, 146(730): 1999-2049, <https://doi.org/10.1002/qj.3803>

**Citation:** LI Cai-ling, BAI Lan-qiang, YU Xiao-ding, et al. A Brief Discussion on the High-impact Cold-season Tornado Outbreak During 10-11 December 2021 in the United States [J]. *Journal of Tropical Meteorology*, 2022, 28(2): 252-260, <https://doi.org/10.46267/j.1006-8775.2022.019>